

A STUDY ON THE EFFECT OF COLLAGEN FIBER ORIENTATION ON MECHANICAL RESPONSE OF SOFT BIOLOGICAL TISSUES

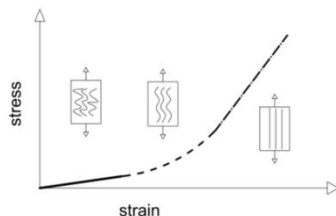
Farshid Fathi*, Shahrokh Shahi, Soheil Mohammadi

School of Civil Engineering, College of Engineering, University of Tehran, Tehran, Iran

Article history
Received
14 February 2015
Received in revised form
15 April 2015
Accepted
31 May 2015

*Corresponding author
farshid.fathi@ut.ac.ir

Graphical abstract



Abstract

Extensive research has been performed in the past decades to study the behavior of soft biological tissues in order to reduce the need for practical experiments. The applicability of these researches, particularly for skin, ligament, muscles and the heart, brings up its importance in various biological science and technology disciplines such as surgery and medicine. Softness and large deformation govern the behavior of soft materials and prohibit the use of small strains solutions in finite element method.

In this work, the focus is set on a strain energy function which has the advantage of accurately representing the behavior of a variety of soft tissues with only a few parameters in a finite element approach. The numerical results are verified with a set of tensile experiments to demonstrate the performance of the proposed model. The parameters include the matrix and collagen bundles and their orientation. Different cases are analyzed and discussed for better prediction of different soft tissue responses.

Keywords: Soft biological tissue, large deformation, finite element method, collagen

© 2015 Penerbit UTM Press. All rights reserved

1.0 INTRODUCTION

Investigation of soft biological tissues has a very long background. The distinct behavior of this group of material and its role in human life gives it a significant importance that encourages many researchers to put their attitude in this field in order to achieve better understanding of their mechanical response, based on simplified or comprehensive theories.

Histologically, the macroscopic mechanical properties of soft biological tissues, like any other solids with micro-scale structure, are affected by microscopic responses. The soft tissues are composed of collagen fibers and ground matrix. The substructure of collagen includes tropocollagens that gather together and make fibrils. Then, bundles of fibrils construct collagen fibers. Collagen has the most load carrying capacity in a soft tissue [1,2]. Collagen is structurally woven in helical patterns and it cannot bear loads (it is negligible in primary region) until it is partially erected and gets along with the loading direction. Afterwards, it

becomes a firm rod and its bearing capacity increases rapidly. This behavior makes the stress-stretch response to be a so called J-shaped curve. It increases significantly when the fibers are mobilized. In the first part of the curve, the main load carrier is the ground matrix [3]. The procedure can be followed in Figure 1.

The soft tissues are generally assumed to be incompressible. Application of this property is generally performed by separating the volumetric and the isochoric parts. The volumetric part comprises a pseudo penalty method to impose the incompressibility condition with the aid of the bulk modulus. For further information on formulation of incompressibility, see Bonet and Wood [4].

One of the earliest works that pushed researchers forward and made a fundamental platform for further developments was reported by Fung [5]. He proposed a hyperelastic model with an exponential strain energy function under the quasi-static loading assumption. Then, many other strain functions were proposed with

different assumptions to model the anisotropic nature of tissue due to the presence of collagen [6-8].

the aortic heart valve [9] or to include the effects of damage [7] or viscosity in soft tissues [8].

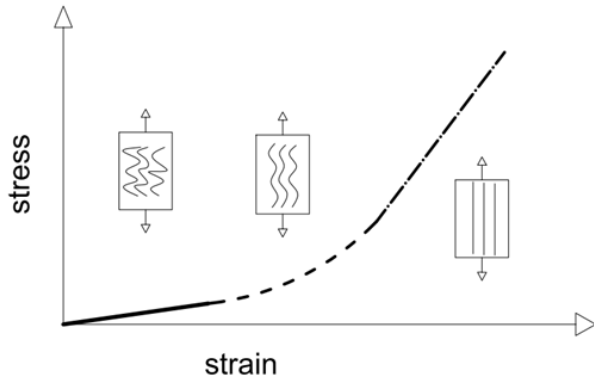


Figure 1 Schematic illustration of fiber response in various levels of loading

Orientation of fibers acts an important role in mechanical response of fiber reinforced materials. It is directly related to histological information of the tissue. For cases such as ligaments and tendons only one preferred direction exists and is aligned with fibers, whereas in cases like arterial walls and skin, the orientation is complicated, and two or three different directions of fibers have to be considered in the formulation.

Holzapfel et al.[3] used the quadratic form of the exponential type $(\exp(c_2[\bar{I}_4 - 1]^2) - 1)$ in terms of, \bar{I}_4 and \bar{I}_6 for different fibers of arterial walls [3]. In the recent decade, new SEFs have been proposed for better estimation of behavior for special cases such as

2.0 RESULTS AND DISCUSSION

2.1 Hyperelastic Strain Energy Function

An arbitrary body in the material configuration is characterized by \mathbf{X} and in the current configuration by \mathbf{x} . The nonlinear deformation mapping from \mathbf{X} to \mathbf{x} , $d\mathbf{x} = \mathbf{F}d\mathbf{X}$, is defined by the deformation gradient $\mathbf{F}(\mathbf{X}) = \nabla \varphi_t(\mathbf{X})$, where the parameter φ_t is the mapping operator and the Jacobian $J(\mathbf{X}) = \det \mathbf{F}(\mathbf{X}) > 0$. The right Cauchy tensor is defined as, $\mathbf{C} = \mathbf{F}^T \mathbf{F}$ which is used to define the second Piola-Kirchhoff stress, $\mathbf{S} = 2\partial_C \hat{\psi}(\mathbf{C})$. Moreover, the principal invariants of the second order tensor \mathbf{C} are presented as, $I_1 = \text{tr} \mathbf{C}$, $I_2 = \text{tr}[\mathbf{C}^2]$, $I_3 = \det \mathbf{C}$.

The structural tensor \mathbf{M} is used to define the pseudo-invariants for considering the anisotropy generated by fibers, $\mathbf{M} = \mathbf{a} \otimes \mathbf{a}$, where \mathbf{a} is the unit vector along the fiber direction. The pseudo-invariant I_4 for the single family of fiber is then defined as, $I_4 = \text{tr}[\mathbf{C}\mathbf{M}]$.

The SEF proposed by Balzani et al.[6] for abdominal aorta is adopted here. The first term is the generalized Neo-Hookean term to represent the isotropic matrix and the second term prohibits the volume change in the case of nearly incompressible material. The anisotropic part is characterized by fibers.

$$\psi^{iso} = c_1 \left(\frac{I_1}{I_3^{1/3}} - 3 \right) + \varepsilon \left(I_3^\gamma + \frac{1}{I_3^\gamma} - 2 \right), \quad c_1 > 0, \quad \varepsilon > 0, \quad \gamma > 1. \tag{Eq. 1}$$

$$\psi^{aniso} = \begin{cases} \sum_{a=1}^2 [\alpha_1 (I_4^{(a)} - 1)^{\alpha_2}] & \text{for } I_4^{(1)} \geq 1 \wedge I_4^{(2)} \geq 1, \\ \alpha_1 (I_4^{(1)} - 1)^{\alpha_2} & \text{for } I_4^{(1)} \geq 1 \wedge I_4^{(2)} < 1, \\ \alpha_1 (I_4^{(2)} - 1)^{\alpha_2} & \text{for } I_4^{(1)} < 1 \wedge I_4^{(2)} \geq 1, \\ 0 & \text{for } I_4^{(1)} < 1 \wedge I_4^{(2)} < 1. \end{cases} \tag{Eq. 2}$$

The second Piola-Kirchhoff is derived as:

$$\mathbf{S}^{iso} = 2 \frac{\partial \psi^{iso}}{\partial \mathbf{C}} = 2c_1 \left(\frac{\mathbf{1}}{I_3^{1/3}} - \frac{1}{3} \frac{I_1 \mathbf{C}^{-1}}{I_3^{1/3}} \right) + 2\varepsilon \gamma (I_3^\gamma - I_3^{-\gamma}) \mathbf{C}^{-1} \tag{Eq. 3}$$

$$\mathbf{S}^{aniso} = \begin{cases} \sum_{a=1}^2 2\alpha_1\alpha_2(\bar{I}_4^a - 1)^{\alpha_2-1} J^{-2/3} \mathbf{M}^a & \text{for } \bar{I}_4^1 \geq 1 \wedge \bar{I}_4^2 \geq 1, \\ 2\alpha_1\alpha_2(\bar{I}_4^a - 1)^{\alpha_2-1} J^{-2/3} \mathbf{M}^1 & \text{for } \bar{I}_4^1 \geq 1 \wedge \bar{I}_4^2 < 1, \\ 2\alpha_1\alpha_2(\bar{I}_4^2 - 1)^{\alpha_2-1} J^{-2/3} \mathbf{M}^2 & \text{for } \bar{I}_4^1 < 1 \wedge \bar{I}_4^2 \geq 1, \\ 0 & \text{for } \bar{I}_4^1 < 1 \wedge \bar{I}_4^2 < 1. \end{cases} \quad \text{where } \mathbf{M}^a = \left[\mathbf{M}^a - \frac{1}{3} I_4^a \mathbf{C}^{-1} \right] \quad (\text{Eq. 4})$$

By further derivation with respect to the right Cauchy tensor \mathbf{C} , the so-called elasticity tensor can be derived. (see Appendix).

Since the fibers do not resist in compression, the tensile test is performed, where the stretch has a value more than one. Therefore, initiation of load bearing in helically shaped fibers can be considered in formulation of the anisotropic part of SEF by subtracting a constant parameter around 1 in the exponential term from the pseudo invariant. Hence, $(I_4^{(1)} - 1)$ utilized in the SEF.

Now, the focus is set on a specific parameter, which has a significant effect on the mechanical response of the soft tissues and it is the angle of fiber orientation. This parameter is defined within the unit vector, a_0 , and is entered in formulation by the generalized new invariants. It can be obtained from the unit vector of fiber direction a_0 and the stretch λ , ($\text{tr}[\mathbf{CM}] \propto a_0 \cdot \mathbf{C} \cdot a_0 \propto \lambda_{a_0}^2$), demonstrating the amount of elongation in the preferred direction.

2.2 Verification and Numerical Example

To illustrate the applicability of the proposed SEF, the finite element numerical results are compared with available experimental tests. As an example, an abdominal aorta of the human cadaver is considered. It is separated into layers and the middle, called media, which is used in tensile tests. Other layers are intima and adventitia but the focus is set on media, which has the most significant role among the arterial layers and a high strength ability to resist high circumferential and longitudinal loads. The schematic illustration of the tissue samples of the arterial wall is presented in Figure 2, and the material parameters are shown in Table 1.

Table 1 Material parameters

c_1 (kPa)	ε (kPa)	γ	α_1 (kPa)	α_2
13.5	10	20	10^{14}	20

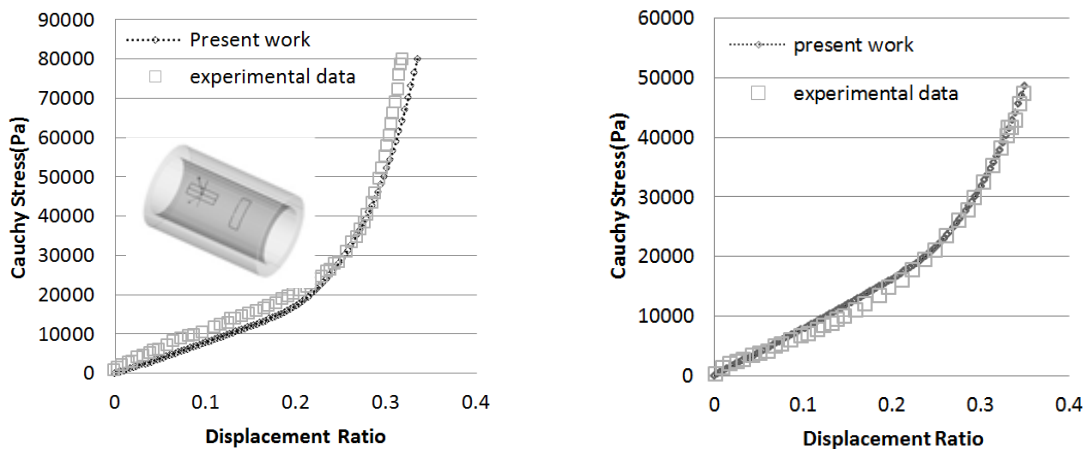


Figure 2 Validation of the model. Comparison of the present results with the experimental data for circumferential (left) and longitudinal (right) oriented strips. The angle between collagen families and the direction of loading in circumferential direction is 43.39°, reported in Balzani et al. (2006).

A large deformation finite element analysis based on the developed formulation is performed, The results are compared with the experimental data of Balzani et al. [6] in Figure 2, which shows a good agreement.

The numerical procedure of fiber alignment is performed several times with different angles between fiber families and the axis of loading to

demonstrate the dependency of response to the distribution of fibers in the direction of loading axis, as illustrated in Figure 3 for circumferential or longitudinal stripped samples. Both samples are subjected to the same uniaxial loading. The results are illustrated in Figure 4.

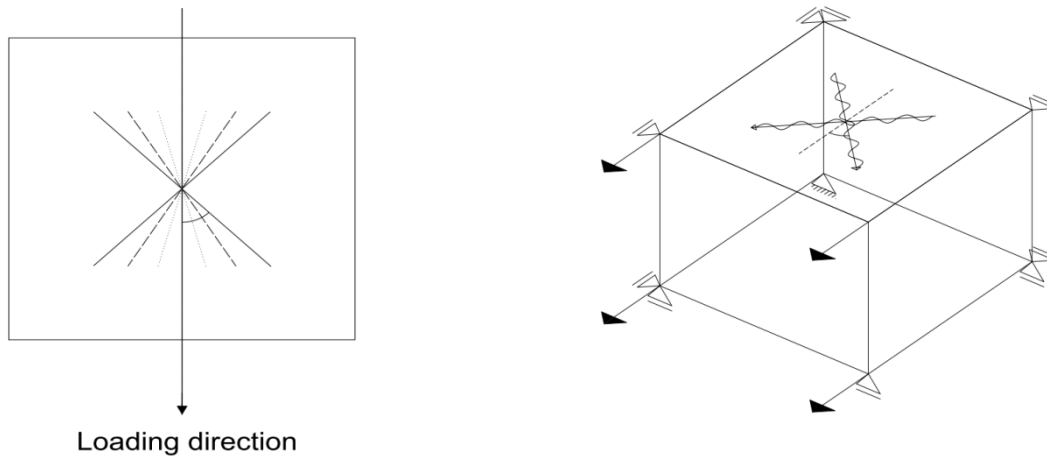


Figure 3 Schematic illustration of fiber orientation in different angles to demonstrate the dependency of mechanical response to the angle.

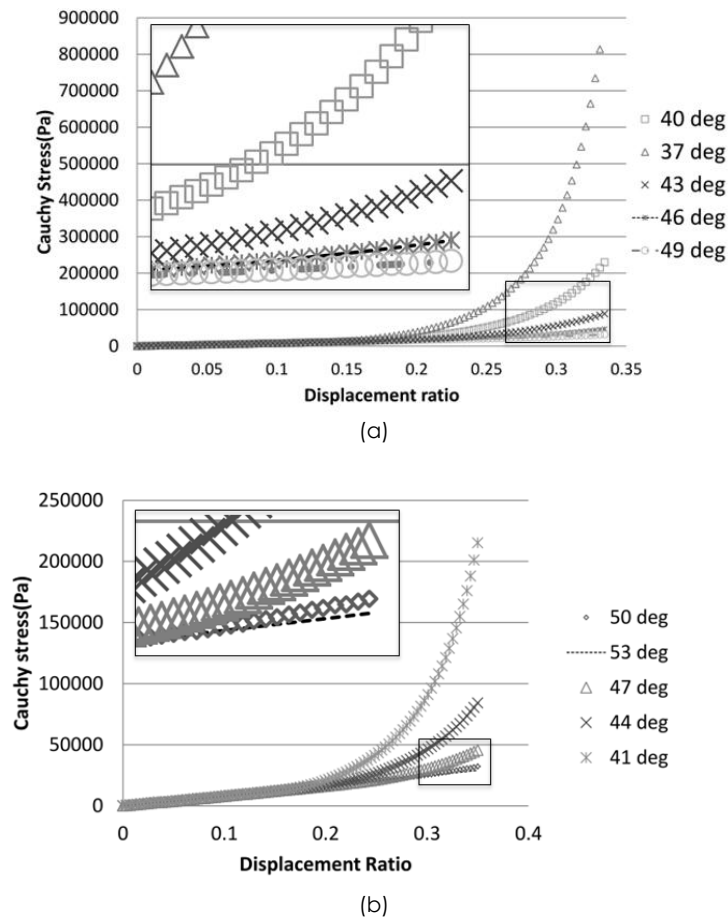


Figure 4 Effect of fiber orientation on the mechanical response of circumferential (a) and longitudinal (b) sample strips

It is evident in Figure 4 that the dependency of mechanical response to the fiber orientation in higher angles (more dispersed) is mostly related to the matrix and less variation is observed. It is also evident that in low values (more coherent orientation) a highly significant effect is observed in the mechanical response in both samples. Particularly, in any specific deformation, very high variation of stress can be reached with a little alteration of angle. It means that any significant projection of vectors which characterize the fiber directions will generate substantially higher stresses and more strength and durability. With a limit analysis, it can be deduced that when the angle " β " between the fiber vector and loading direction approaches zero ($\lim_{\beta \rightarrow 0}(\cos \beta) = 1$),

the biggest projection and the highest strength are reachable. Thus, fibers play a significant role in the mechanical response in more coherent cases, whereas in dispersed cases, it is the matrix that has the main role because the fibers are not mobilized.

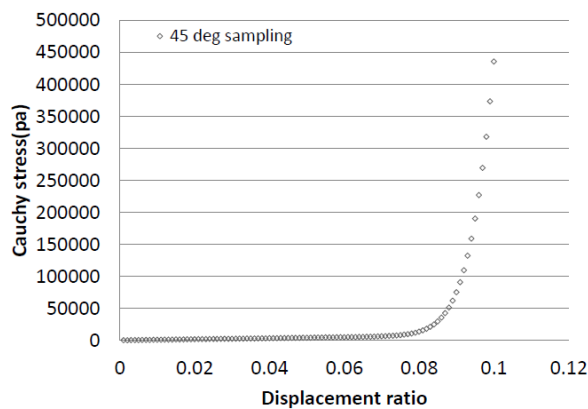


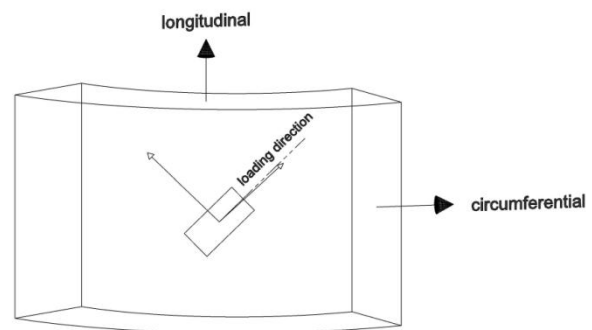
Figure 5 Illustration of the inclined sampling and mechanical response. The angle between loading direction and longitudinal axis is 45°

4.0 CONCLUSION

In this study, the kinematics and large deformation is successfully incorporated within a strain energy function, which shows a good agreement with the experimental data. A comprehensive formulation, based on derivatives of the strain energy function, includes the pseudo invariants, which characterize the elongation in the direction of fibers. The changes in the angle between the families of fibers and the loading direction are studied to determine the significance of this parameter. The density of collagen fibers along the loading direction is the most important parameter in the mechanical response. A direct dependency exists between the number of collagen in the direction of loading and the mechanical response. It means that the bigger the projection of collagen fibers in direction of loading, the more the resistance of the tissue. Thus, the strength of a soft tissue mostly depends on the fiber orientation. In near future, it would be possible to produce artificial tissues

Another numerical example analyzed in this work is the special sampling in 45° with respect to the longitudinal direction. Details are presented in Figure 6. The fiber distribution in this case is the natural orientation reported in Balzani et al. (2006) with respect to circumferential direction [6]. The results of 45° inclined sampling are presented in Figure 6.

Comparing Figure 5 and Figure 6, the significant role of angle of fiber and loading direction is observable. In the inclined sampling case, when the angle of fiber family 1 is $\beta = 1.61^\circ$, the partial alignment with the loading direction ($\beta \rightarrow 0$) allows for higher load bearing, whereas the fiber family 2 is approximately perpendicular to the axis of loading ($\beta = 91.61^\circ$) and does not significantly affect the behavior of the tissue sample. Clearly, the role of fiber as the most load bearing component is evident. It is also observable that in lower displacements, considerable higher stresses are reached.



as natural as reality, so the orientation and accumulation of these fibers will act an important role in tissue engineering.

References

- [1] Fung, Y. C. 1993. Mechanical Properties of Living Tissues, Second ed. Springer, New York Berlin Heidelberg. *Biomechanics*.
- [2] Itskov, M., Ehret, A. E. and Mavrilas, D. 2006. A Polyconvex Anisotropic Strain-Energy Function for Soft Biological Tissues. *Biomechanics and Modelling In Mechanobiology*. 5: 17-26.
- [3] Holzapfel, G. A. 2000. Biomechanics of Soft Tissue. *Computational Biomechanics*.
- [4] Bonet, J. and Wood, R. D. 2008. Nonlinear Continuum Mechanics for Finite Element Analysis. *Cambridge University Press*. Cambridge.
- [5] Fung, Y. C. 1993. Biorheology of Soft Tissues. *Biorheology*. 10: 139-155.
- [6] Balzani, D. Neff, P. Schroder, J. and Holzapfel, G. A. 2006. A Polyconvex Framework for Soft Biological Tissues.

Adjustment to Experimental Data. *International Journal of Solids and Structures*. 43: 6052-6070.

[7] Pena, E. 2011. Prediction of the Softening and Damage Effects with Permanent Set In Fibrous Biological Materials. *Journal of Mechanics and Physics of Solids*. 59: 1808-1822.
 [8] Holzapfel, G. A. and Gasser, T. C. 2001. A Viscoelastic Model for Fiber-Reinforced Composites and Finite Strains:

Continuum Basis, Computational Aspects and Applications, *Computer. Methods in Applied. Mechanics. and Engineering*. 190: 4379-4403.

[9] Shahi, S. and Mohammadi, S. 2013. A Multiscale Finite Element Simulation of Human Aortic Heart Valve. *Applied Mechanics and Materials*. 367: 275-279.

Appendix

The elasticity tensor for the proposed function is derived as:

$$\square^{iso} = 4c_1 \left(-\frac{1}{3} \frac{\mathbf{C}^{-1} \otimes \mathbf{1}}{I_3^{1/3}} - \frac{1}{3} \frac{\mathbf{1} \otimes \mathbf{C}^{-1}}{I_3^{1/3}} + \frac{1}{9} \frac{I_1}{I_3^{1/3}} \mathbf{C}^{-1} \otimes \mathbf{C}^{-1} + \frac{1}{3} \frac{I_1}{I_3^{1/3}} \mathbf{I} \right) + \dots$$

$$4\varepsilon\gamma \left(\gamma I_3^\gamma \mathbf{C}^{-1} \otimes \mathbf{C}^{-1} - I_3^\gamma \mathbf{I} + \gamma I_3^{-\gamma} \mathbf{C}^{-1} \otimes \mathbf{C}^{-1} + I_3^{-\gamma} \mathbf{I} \right)$$
(Eq. 5)

$$\square^{aniso} = \begin{cases} \sum_{a=1}^2 4\alpha_1\alpha_2 \{ (\bar{I}_4^a - 1)^{\alpha_2-1} \frac{1}{3} J^{-2/3} \chi^a + (\alpha_2 - 1)(\bar{I}_4^a - 1)^{\alpha_2-2} J^{-4/3} \xi^a \} & \text{for } \bar{I}_4^1 \geq 1 \wedge \bar{I}_4^2 \geq 1, \\ 4\alpha_1\alpha_2 \{ (\bar{I}_4^1 - 1)^{\alpha_2-1} \frac{1}{3} J^{-2/3} \chi^1 + (\alpha_2 - 1)(\bar{I}_4^1 - 1)^{\alpha_2-2} J^{-4/3} \xi^1 \} & \text{for } \bar{I}_4^1 \geq 1 \wedge \bar{I}_4^2 < 1, \\ 4\alpha_1\alpha_2 \{ (\bar{I}_4^2 - 1)^{\alpha_2-1} \frac{1}{3} J^{-2/3} \chi^2 + (\alpha_2 - 1)(\bar{I}_4^2 - 1)^{\alpha_2-2} J^{-4/3} \xi^2 \} & \text{for } \bar{I}_4^1 < 1 \wedge \bar{I}_4^2 \geq 1, \\ 0 & \text{for } \bar{I}_4^1 < 1 \wedge \bar{I}_4^2 < 1. \end{cases}$$
(Eq. 6)

$$\chi^a = \left[\frac{1}{3} I_4^a \mathbf{C}^{-1} \otimes \mathbf{C}^{-1} - \mathbf{C}^{-1} \otimes \mathbf{M} - \mathbf{M} \otimes \mathbf{C}^{-1} + I_4^a \mathbf{I} \right] \text{ and}$$

$$\xi^a = \left[\frac{1}{9} (I_4^a)^2 \mathbf{C}^{-1} \otimes \mathbf{C}^{-1} - \frac{1}{3} I_4^a \mathbf{C}^{-1} \otimes \mathbf{M} - \frac{1}{3} I_4^a \mathbf{M} \otimes \mathbf{C}^{-1} + \mathbf{M} \otimes \mathbf{M} \right]$$